

A Photometric Study of the Ages and Metallicities of Early-type Galaxies in A 2218

Ian Smail,¹ Harald Kuntschner,¹ T. Kodama,¹ G. P. Smith,¹ C. Packham,² A. S. Fruchter³ & R. N. Hook⁴

¹ Department of Physics, University of Durham, South Road, Durham DH1 3LE

² Isaac Newton Group, Apartado 321, 38780 Santa Cruz de La Palma, Tenerife, Canary Islands, Spain

³ Space Telescope Science Institute, 3700 San Martin Drive, Baltimore, MD21210, USA

⁴ Space Telescope – European Coordinating Facility, European Southern Observatory, Karl-Schwarzschild-Str. 2, D-85748 Garching b. München, Germany

arXiv:astro-ph/0008160v1 10 Aug 2000

SUBMITTED: 9 NOVEMBER 2018

ABSTRACT

We present deep optical and near-infrared imaging of the rich cluster A 2218 at $z = 0.17$. Our optical imaging comes from new multicolour *Hubble Space Telescope* WFPC2 observations in the F450W (B_{450}), F606W (V_{606}) and F814W (I_{814}) passbands. These observations are complemented by deep near-infrared, K_s -band, imaging from the new INGRID imager on the 4.2-m William Herschel Telescope. This combination provides unique high-precision multicolour optical-infrared photometry and morphological information for a large sample of galaxies in the core of this rich cluster at a lookback time of ~ 3 Gyrs. We analyse the $(B_{450} - I_{814})$, $(V_{606} - I_{814})$ and $(I_{814} - K_s)$ colours of galaxies spanning a range of a factor of 100 in K -band luminosity in this region and compare these with grids of stellar population models. We find that the locus of the colours of the stellar populations in the luminous ($\gtrsim 0.5L_K^*$) early-type galaxies, both ellipticals and S0s, traces a sequence of varying metallicity at a single age. At fainter luminosities ($\lesssim 0.1L_K^*$), this sequence is extended to lower metallicities by the morphologically-classified ellipticals. However, the faintest S0s exhibit very different behaviour, showing a wide range in colours, including a large fraction (30%) with relatively blue colours which appear to have younger luminosity-weighted ages for their stellar populations, 2–5 Gyrs. We show that the proportion of these young S0s in the cluster population is consistent with the observed decrease in the S0 population seen in distant clusters when interpreted within the framework of a two-step spectroscopic and morphological transformation of accreted spiral field galaxies into cluster S0s.

Key words: galaxies: elliptical and lenticular – galaxies: stellar content – galaxies: evolution – cluster of galaxies: individual, A 2218

1 INTRODUCTION

Studies using photometric, and more recently spectroscopic, observations of luminous elliptical galaxies in distant clusters have suggested that their luminosity and colour evolution is modest and consistent with passive evolution of stellar populations which are formed at high redshifts, $z > 2$ –4 (Aragon-Salamanca et al. 1993; Ellis et al. 1997; van Dokkum et al. 1998; Kodama et al. 1998; Kelson et al. 2000).

The relatively modest evolution seen in the luminous elliptical population in clusters contrasts with the claims of strong evolution in the morphological mix in these environments, specifically the ratio of S0 (lenticular) to elliptical

galaxies. Using *Hubble Space Telescope* (*HST*) imaging of ten clusters at $z > 0.3$ –0.6, Dressler et al. (1997) have uncovered a rapid increase in the ratio of S0 to elliptical galaxies towards the present day (see also Fasano et al. 2000). Assuming that the elliptical population is static, they interpret this as a strong rise in the S0 population, from 10–20% at $z \sim 0.5$ (6 Gyrs ago) to the 60% seen in present-day rich clusters. This apparent evolution applies to the cluster population brighter than about $0.1L_V^*$.

By including information from spectroscopic observations of galaxies in ten clusters, Poggianti et al. (1999) proposed that the build-up of S0 galaxies identified by Dressler et al. (1997) resulted from the morphological transforma-

tion into lenticulars of accreted field spiral galaxies. They further suggested that the presence of a large population of red, apparently passive, galaxies with late-type morphologies in the clusters, along with absence of blue S0 galaxies, indicated that the morphological transformation occurs on a longer timescale than the decline in the star formation rates of the accreted field galaxies (see also Kodama & Smail 2000). Thus they proposed that the galaxies first suffered a decline in their star formation (probably resulting from stripping of their gas reservoirs as they encounter the dense intracluster medium within the cluster potential) and only then had their morphological appearance transformed (perhaps by a completely separate process, e.g. Moore, Lake & Katz 1998).

Nevertheless, if the morphological transformation occurs on a timescale of $\lesssim 2$ –3 Gyr after the galaxy's entry into the cluster it may still be possible to identify subtle signatures of this previous activity in the S0 population. Direct comparisons of the estimated stellar population ages for the S0 and elliptical populations can be particularly powerful in this respect. When comparing the composite spectra of the S0 and elliptical populations in three clusters at $z = 0.3$, Jones, Smail & Couch (2000) found no significant differences in the inferred luminosity-weighted ages of the stellar populations in the two classes at a median luminosity of $0.6L_V^*$ and concluded that this supported the two-step transformation model discussed above. A similar degree of homogeneity between the cluster E and S0 galaxies was reported by Ellis et al. (1997) from their study of the restframe ($U - V$) colours of early-type galaxies in three clusters at $z \sim 0.5$, although again the strongest constraints were on the more luminous galaxies, $\gg 0.2L_V^*$. However, a more detailed spectral-line analysis of individual lenticular and ellipticals in Fornax (Kuntschner 2000) has suggested that, in this cluster at least, the low luminosity lenticulars ($\lesssim 0.1L_V^*$) exhibit typically younger luminosity-weighted ages for their stellar populations than the ellipticals (see also Jorgensen 1999).

Work on the relative ages of cluster ellipticals and lenticulars continues using new combinations of spectral line indices to break the degeneracy between age and metallicity (Worthey 1994; Vazdekis & Arimoto 1999; Kuntschner 2000). At higher redshift such studies can be observationally expensive, requiring relatively large amounts of 4- and 8-m time and efficient multi-object spectrographs (Kelson et al. 1997; Jorgensen et al. 1999; Ziegler et al. 2000). However, recent developments in stellar population modelling (e.g. Vazdekis et al. 1997; Kodama & Arimoto 1997; Bruzual & Charlot 2000) have suggested that it may be possible to break the Age–Metallicity degeneracy using observationally cheaper photometric analyses if it includes both optical *and* near-infrared (H or K) photometry (an idea originally proposed by Aaronson 1978, see Peletier & Balcells 1996 for an early demonstration). In this paper we explore this possibility using new, high-quality observations of the galaxy population in the core of the rich cluster A 2218 ($z = 0.17$) from *HST* and the new INGRID near-infrared imager on the William Herschel Telescope (WHT). We derive precise optical and optical-infrared colours and morphologies for a large sample of galaxies across a 6 magnitude range in near-infrared luminosity down to $K_s = 19$ ($0.02L_K^*$) in this field and compare these to the predictions of the latest stellar evolutionary models. We also compare the constraints we

derive for individual galaxies with the recent spectroscopic study of A 2218 by Ziegler et al. (2000). We discuss our observations and their reduction in the next section, present our results in §3 and our conclusions in §4. Throughout we assume $q_0 = 0.5$ and $h = 0.5$ in units of $100 \text{ km s}^{-1} \text{ Mpc}^{-1}$. In this cosmology the look-back time to A 2218 is 3 Gyr, the angular scale at the cluster is $1'' \equiv 4.3 \text{ kpc}$ and $K_s^* = 14.8$ (adopting $M_K^* = -25.7$).

2 OBSERVATIONS, REDUCTION AND ANALYSIS

2.1 *HST* Optical Imaging

The *HST*^{*} imaging analysed here was obtained as part of the Early Release Observations (ERO) from *WFPC2* after the SM-3a servicing mission in January 2000. The observations comprise 5 orbits in each of the F450W, F606W and F814W passbands, giving total integration times of 11.0 ks, 10.0 ks and 12.0 ks respectively. These exposures were each broken into 1000's sub-exposures which were spatially offset from each other by sub-pixel shifts to allow drizzle-reconstruction of the frames to recover some of the information lost due to the undersampling of the *HST* PSF by the *WFC* pixel arrays.

The individual images were processed using the standard *WFPC2* data pipeline and subsequently combined and cleaned of cosmic ray and other artifacts using DRIZZLE and related software (Fruchter & Hook 1997) as implemented in IRAF/STSDAS. The final *WFC* images have an effective resolution (FWHM) of $0.17''$, $0.05''$ -sampling and cover a field of 5.0 sq. arcmin . We adopt the photometric calibration of Holtzman et al. (1995) as given on the STScI web pages to calculate magnitudes in the Vega-based $B_{450}/V_{606}/I_{814}$ system. We use an average Gain Ratio of 1.988 for the three *WFC* chips, but note that for the colours based on the *HST* photometry the adopted Gain Ratio cancels out, and for the *HST*–INGRID colours the uncertainty it introduces is much smaller than the calibration error of the ground-based photometry. The 3σ point source sensitivities in the two passbands are then: $B_{450} = 28.8$, $V_{606} = 29.0$ and $I_{814} = 28.1$. At the redshift of A 2218 these filters sample the cluster population in passbands roughly equivalent to restframe U , V and R . We show a true-colour representation of the cluster as seen in the *HST* imaging in Figure 1.

2.2 INGRID Near-infrared Imaging

Our near-infrared observations come from the new INGRID imager on the 4.2-m WHT[†] (Packham et al. 2000). These observations were obtained in commissioning time during March 22–23, 2000. INGRID comprises a 1024^2 HAWAII-2

^{*} This paper is based upon observations obtained with the NASA/ESA *Hubble Space Telescope* which is operated by STScI for the Association of Universities for Research in Astronomy, Inc., under NASA contract NAS5-26555.

[†] Based on observations made with the William Herschel Telescope operated on the island of La Palma by the Isaac Newton Group in the Spanish Observatorio del Roque de los Muchachos of the Instituto de Astrofisica de Canarias

Fig1.jpg

Figure 1. A true colour *HST* image of the core of A 2218 composed from the F450W (blue), F606W (green) and F814W (red) images. North is up and east is to the left. We identify the galaxies employed in our study using the numbering scheme given in Table 1. The coordinates are measured relative to the position of the central cD galaxy (#301, $\alpha = 16^h 35^m 49\rlap{.}^s 31$, $\delta = +66^\circ 12' 44\rlap{.}^s 7$ (J2000)).

array at the bent-Cassegrain focus of the WHT, providing a 4.13 arcmin field of view with $0.242''/\text{pixel}$ sampling.

Our exposures consist of a total of 8.3 ks integration in the K_s filter obtained under photometric conditions in $\sim 0.6\text{--}0.8''$ seeing. An additional 9.1 ks of J -band imaging was also obtained and we discuss this elsewhere (Smith et al. 2000). The K_s frames consist of individual 20 s exposures which are co-added in hardware. These were reduced in a standard manner using a smoothed illumination correction derived from all the K_s frames obtained during the night and then a local sky correction constructed from a running median of frames around a particular science frame. The frames were then aligned using integer-pixel shifts and combined using a cosmic-ray rejection algorithm to produce a

final frame. The photometric calibration of these frames is obtained from exposures of UKIRT Faint Standards interspersed between the science observations. We estimate that our absolute calibration is good to 0.03 mags (including the uncertainty in the transformation from K to K_s for the faint standards, Persson et al. 1998). The final stacked K_s -band frame (approximately restframe H -band) has a 3σ point-source sensitivity, within the seeing disk, of $K_s = 22.0$ and seeing of $0.75''$.

2.3 Galaxy Catalogue and Colours

To undertake our analysis we construct a K_s -selected galaxy catalogue. This achieves two goals – it minimises our sen-

sensitivity to differences in the previous star formation histories of the galaxies we are studying, and as the K_s frames have effectively the shallowest limit, selecting in the K_s -band guarantees a sample with the most uniform optical-infrared colours and errors. Looking at the model grids shown in Figure 3 we can see that to differentiate between different stellar populations we require typical photometric errors of better than ≤ 0.1 mag in $(I_{814} - K_s)$. This imposes an effective K_s -band magnitude limit of $K_s < 19.0$ on our sample, equivalent to $M_{K^*} + 4.2$ mags or roughly $M_K = -21.5$ for early-type galaxies in A 2218.

We therefore ran SExtractor (Bertin & Arnouts 1996) on the final K_s frame using a detection criteria of 10 pixels above the $\mu_{K_s} = 21.2$ mag arcsec $^{-2}$ isophote (1.5σ). To determine the total magnitudes of galaxies on this frame we use the BEST_MAG estimate from SExtractor and confirm that this provides a reliable ($\delta K_s \leq 0.05$) estimate of the total magnitudes using large-aperture photometry of several bright, isolated galaxies in the field. The SExtractor catalogue provides a list of 106 sources within the joint *WFPC2*-INGRID field down to our adopted limit of $K_s = 19$. We discard 10 sources as being stellar on the basis of their morphologies in the F814W frame, a further 8 due to crowding (another $K_s < 19$ source within 1–2 half-light radii) and 7 which exhibit gravitationally-lensed morphologies which obviously discount them from our analysis of the cluster population (an optical-infrared photometric analysis of the arcs and arclets seen in A 2218 will be presented by Smith et al. 2000). This leaves us with a final sample of 81 candidate cluster galaxies which are brighter than $K_s = 19$ and relatively uncrowded, these galaxies are identified on Figure 1.

Morphologies of the galaxies in the A 2218 field were kindly provided by Prof. Warrick Couch based on the existing *WFPC2* imaging in the F702W (R_{702}) passband presented by Kneib et al. (1996). These morphologies are on the revised Hubble scheme as used by the MORPHS project (Smail et al. 1997). We have chosen to use visual classifications for our analysis, rather than profile fitting, as all of the claims for morphological evolution of the galaxy populations of distant clusters have used visual estimates of the morphologies. Therefore any signatures of this evolution should appear in visually classified samples. The roll-angle and field centre for the earlier F702W observations were different from the ERO observations analysed here and so there is a slight mismatch in the field coverage between the two datasets. This results in 15 galaxies out of the 81 galaxies in our final $K_s < 19$ sample lacking morphologies. Morphological classification of these galaxies was undertaken by one of us (IRS) from the F814W frame. These galaxies are identified by ID's of 4000 and above in Table 1. The morphologies of the $K_s < 19$ sample break down as: E: 31; E/S0: 3; S0: 28; Sa: 5; late-type spirals: 14. The core of A 2218 thus exhibits an observed S0-to-E ratio, $N_{S0}/N_E \sim 1$, close to that expected from the evolutionary rate proposed by Dressler et al. (1997), and a large deficit of S0 galaxies compared to the ratio seen in local clusters, $N_{S0}/N_E \sim 2.3$. Within the framework of the S0-transformation model we would expect that roughly half of the S0 population we see in A 2218 had their morphologies transformed since $z \sim 0.5$.

To determine representative colours for these galaxies we have chosen to measure photometry from the seeing-

matched frames within an aperture whose radius is three times the half-light radius of the galaxy. The half-light radii, r_{hl} , we quote are simply the radius of a circle containing half the total light of a galaxy on the F814W frame. To estimate the total magnitudes we use the SExtractor BEST_MAG measurements and correct these to ‘total’ magnitudes using 8.0''-diameter aperture photometry of isolated early-type galaxies on the frame. This correction amounts to -0.05 ± 0.01 mag. A comparison of our half-light radii with the effective radii published by Jorgensen et al. (1999) and Ziegler et al. (2000) from their analyses of the *HST* F702W-band frame shows reasonable agreement, $\lesssim 20\%$ scatter. The median half-light radius reaches 0.4'' (equivalent to the ground-based seeing) by our limit of $K_s = 19$. For the galaxies with half-light radii below 0.4'' (14/81) we have chosen to use a fixed aperture of 2.4'' diameter.

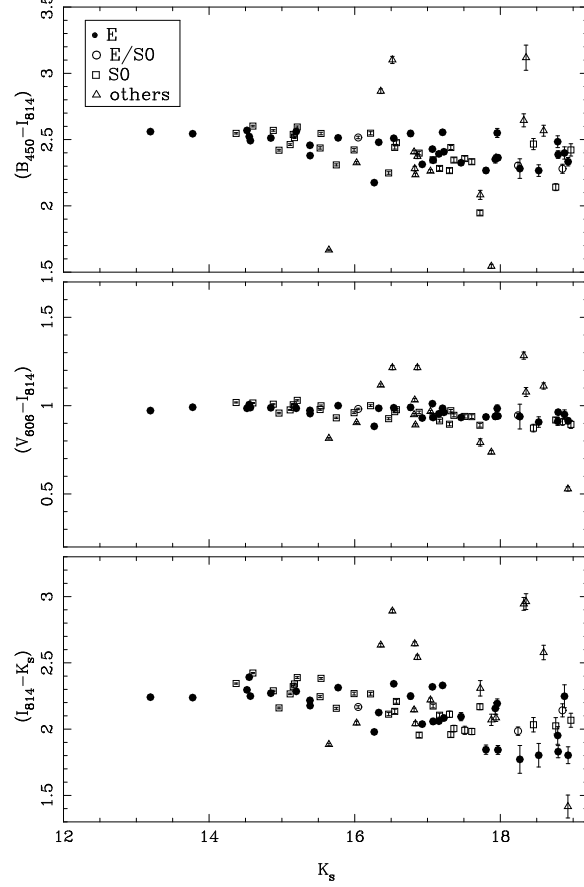


Figure 2. Colour-magnitude diagrams for the $K_s < 19$ sample showing their $(B_{450} - I_{814})$, $(V_{606} - I_{814})$ and $(I_{814} - K_s)$ colours as a function of total K_s magnitude. The points are coded on the basis of their optical morphology given in the key. Note the tight sequences exhibited by the colours of the early-type galaxies, especially in $(V_{606} - I_{814})$.

To measure the colours of the galaxies we aligned and resampled the *HST* frames to the coordinate system defined by the INGRID K_s frame to a tolerance of $\ll 0.1''$. We then matched the effective PSF on the *HST* and ground-based frames using an iterative gaussian-convolution technique based on the PSF profiles within the same $3r_{hl}$ radius used in our analysis. For each galaxy we measure the $(B_{450} - I_{814})$, $(V_{606} - I_{814})$ and $(I_{814} - K_s)$ colours within the adopted apertures. To judge the sensitivity of our colours to

the PSF correction we have reanalysed our frames using PSF convolutions at either extreme of the range of acceptable values and have determined that the $(I_{814} - K_s)$ colours, which have the strongest sensitivity to this correction, vary by less than 0.02 mags. We have also remeasured the colours using apertures which are twice the half-light radii and determine that the distribution of the early-type population on the colour-colour planes does not significantly alter, with systematic changes in the colours of < 0.02 mags.

We list the aperture photometry for our sample, along with the errors estimated from photon-counting statistics and the variance of the sky background, our best-estimate of the total K_s magnitudes and the half-light radii in Table 1. Table 1 also gives the positions of all the galaxies, this astrometry is tied to the APM coordinate system and has positional accuracy of $\lesssim 0.5''$ rms. We illustrate the colour-magnitude relations for the galaxies in the different passbands in Figure 2. The estimated galactic extinction for this field from Schlegel et al. (1998) is $E(B - V) = 0.024$, giving $E(B_{450} - I_{814}) = 0.058$, $E(V_{606} - I_{814}) = 0.034$, $E(I_{814} - K_s) = 0.038$ and $A_K = 0.01$. We correct all colours for extinction but have not corrected the total K_s -band magnitudes. Adopting the Burstein & Heiles (1982) estimate of the extinction reduces the reddening corrections by 25% – or at most 0.01 mags.

2.4 Archival Spectroscopy

We expect that field galaxies are likely to comprise a relatively modest fraction of our K_s -selected sample given the richness and redshift of the cluster we are observing (especially for the early-type galaxies). Nevertheless, we have searched for spectroscopic confirmation of the membership of the galaxies in our sample. The primary sources for this information are Le Borgne, Pello & Sanahuja (1992), Jorgensen et al. (1999) and Ziegler et al. (2000). We find a total of 33 of the 81 galaxies in our sample have spectroscopic redshifts. We list the identifications for these galaxies and their redshifts in Table 1, following the naming convention from NED[‡].

Of the 33 spectroscopically identified galaxies only two are non-members, and only one of these (#4010) has an early-type morphology – indicating a field contamination of 3% (for the typically brighter galaxies above the spectroscopic limits). The observed colours of #4010 project it onto the sequence of metal-rich, luminous ellipticals in the cluster. Three other much fainter ellipticals also appear in this region (identified by their large photometric errors in Fig. 4c) and we suggest that these probably represent background field galaxies, although this requires spectroscopic confirmation. The morphological breakdown of the spectroscopic members is: 17/31 E's, 1/3 E/S0's, 13/28 S0's and 2/5 Sa's, showing that we have confirmed membership for roughly 40% of the early-type galaxies in our field. In addition, 14 of the early-type galaxies in our sample have high signal-to-noise, moderate resolution spectroscopy available

[‡] The NASA/IPAC Extragalactic Database (NED) is operated by the Jet Propulsion Laboratory, California Institute of Technology, under contract with the National Aeronautics and Space Administration.

Table 2. The sensitivity to age and metallicity of the colours used in our analysis. The rate of change of colour is determined for $2 < T(\text{Gyr}) < 10$ and $-0.7 < [\text{M}/\text{H}] < 0.0$. The ratio, $(d(\text{col})/d[\text{M}/\text{H}])/(d(\text{col})/d \log T)$, is also shown in the final column.

Colour	$d(\text{col})/d[\text{M}/\text{H}]$	$d(\text{col})/d \log T$	Ratio
$(B_{450} - I_{814})$	0.53	0.56	0.96
$(V_{606} - I_{814})$	0.15	0.22	0.67
$(I_{814} - K_s)$	0.76	0.45	1.73

from Ziegler et al. (2000). We discuss these galaxies in more detail in the next section.

2.5 Stellar Population Models

We compare the observed colours of the galaxies with the predictions from Bruzual & Charlot's (2000) population synthesis code. The single stellar population (SSP, a stellar population with a single metallicity and age) model grids are calculated for six different metallicities ($[\text{M}/\text{H}] = -2.3, -1.7, -0.7, -0.4, 0.0$, and $+0.4$) and eight ages ($T = 1, 1.5, 2, 3, 5, 7, 10, 15$ Gyrs). We assume a Salpeter (1955) initial mass function ($x = 1.35$) with lower and upper mass cut-offs of 0.1 and 100 M_\odot . The colours are calculated in the observer's frame at the cluster redshift ($z = 0.17$) by redshifting the SSP spectra and convolving these with the filter response functions.

As shown in Figure 3, the Age–Metallicity degeneracy can be broken by combining a rest-frame optical colour and a rest-frame optical-infrared colour. This is because the optical-infrared colour (e.g. $(I_{814} - K_s)$) of an old stellar population (> 1 Gyr) is primarily determined by the temperature of the red giant branch which is much more sensitive to the metallicity than the age of the stellar populations (Table 2). In contrast, an optical colour (e.g. $(V_{606} - I_{814})$) is sensitive to *both* age and metallicity in accordance with the predictions of Worthey's (1994) 2/3 law. Bluer optical colours which sample the restframe near-ultraviolet (e.g. $(B_{450} - I_{814})$ at $z = 0.17$) are slightly more sensitive to the metallicity than the 2/3 law suggests, since this colour brackets the rest-frame 4000Å break which is sensitive to metal lines (e.g. Fe and Ca HK). Therefore the best combination to break the Age–Metallicity degeneracy for a cluster at $z \sim 0.2$ is $(V_{606} - I_{814})$ versus $(I_{814} - K_s)$.

3 RESULTS AND DISCUSSION

We show the three colour–magnitude diagrams for our sample in Figure 2. These illustrate the wide range in luminosity covered in our analysis, nearly 6 magnitudes, with the elliptical and lenticular galaxies evenly spread across this range, except for the brightest two galaxies which are both ellipticals. This figure also shows the relatively homogeneous colours of the majority of the galaxies in our sample. The combined elliptical and lenticular sample exhibits a scatter around their mean relations of 0.11 mag in $(B_{450} - I_{814})$, 0.17 mag in $(I_{814} - K_s)$ and a mere 0.03 mag in $(V_{606} - I_{814})$. However, this scatter is still significantly larger than the mean errors in these colours: $\delta(B_{450} - I_{814}) = 0.02$,

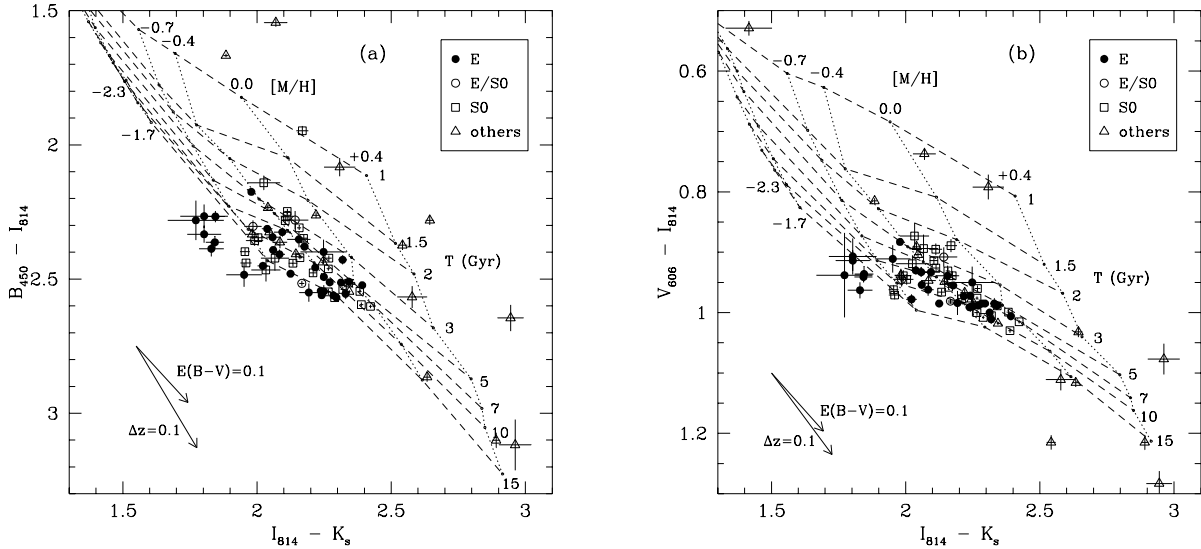


Figure 3. Colour-colour diagrams for the $K_s < 19$ sample comparing the $(B_{450} - I_{814})$ and $(V_{606} - I_{814})$ versus $(I_{814} - K_s)$ planes. The points are coded on the basis of their optical morphology as given in the key. The two vectors show the effects on the galaxy colours of increasing the internal reddening and increasing redshift (assuming an early-type spectral energy distribution).

$\delta(I_{814} - K_s) = 0.03$ and $\delta(V_{606} - I_{814}) = 0.01$. As we show next, the high precision of our photometry of the early-type galaxies in A 2218 means that we can analyse the small scatter shown in their colours to uncover differences in their stellar populations.

In Figure 3 we show the two colour-colour diagrams based on the $(B_{450} - I_{814})$ and $(V_{606} - I_{814})$ comparisons with $(I_{814} - K_s)$. We overplot on this figure the grid of models for a range of ages and metallicities (as described in §2.5). We indicate in both panels the effects on the observed colours of increasing reddening and redshift (for early-type SEDs). The redshift vector suggests that the fainter end of our sample could suffer field contamination from foreground low-luminosity, but metal-rich, early-type galaxies. This combination of properties is sufficiently rare and the foreground volume small enough that we do not expect contamination to be a major problem in our analysis.

A comparison of the model grids and the observations in Figure 3 shows good agreement between the regions of the colour-colour plane populated by the observations and those where galaxies are expected to lie on the basis of the stellar population models. However, comparing the ‘orthogonality’ of the age and metallicity tracks on the two colour-colour planes in Figure 3 we can see that the $(V_{606} - I_{814})$ grid provides a better differentiation between age and metallicity than $(B_{450} - I_{814})$ as expected from the discussion in §2.5. Hence, for the remainder of our analysis we will concentrate on the $(V_{606} - I_{814})$ – $(I_{814} - K_s)$ colour-colour plane and compare the detailed distribution of the galaxies on it to the model tracks.

The dominant feature in the $(V_{606} - I_{814})$ panel in Figure 3 (and also shown by the $(B_{450} - I_{814})$ plot) is a tight locus of points in the region of the grid corresponding to the oldest and most metal rich stellar populations. These galaxies are typically the brightest early-type galaxies in the cluster (Fig. 2). Their locus traces what appears to be a metallicity sequence – spanning a range of ~ 0.5 dex in $[M/H]$ –

at a single age (~ 7 Gyr – although the uncertainty in the metallicities and the relative calibration of the colours and grids means that the reader should view the ages as defined on a relative rather than an absolute scale). This can be more clearly seen in Figure 4, which illustrates the $(V_{606} - I_{814})$ – $(I_{814} - K_s)$ distributions for the morphologically classified elliptical and lenticular galaxies (we place the three E/S0 galaxies into the latter sample). The fainter galaxies (identified by the larger photometric errors) extend this sequence to lower $[M/H]$, but also appear to show a wider spread in ages. Indeed a number of the faintest elliptical galaxies fall just outside the region covered by the model predictions, although their photometric errors are sufficiently large that we do not view this as a major concern. Unfortunately none of these galaxies have spectroscopic information to confirm their cluster membership.

To confirm the reliability of our analysis we compare our results for the 14 galaxies in common with the spectroscopic sample of Ziegler et al. (2000). We note that these galaxies are typically the brighter ones in our sample, with a median magnitude of $K_s = 15.1$, the faintest having $K_s = 16.3$ ($0.25L_K^*$). We find that most of the galaxies are consistent in both analyses with a single age (~ 7 –8 Gyr) and a range of metallicity. However, one galaxy stands out in our sample – #449, the bluest, confirmed elliptical member in Figure 4b – the luminosity-weighted age we derive for the stellar population in this galaxy is a mere 3 Gyr (suggesting that the stellar population which currently dominates the galaxy’s luminosity was formed at a redshift of only $z \lesssim 0.5$). This galaxy also stands out in Ziegler et al.’s analysis as by far the youngest galaxy in the joint sample, with an estimated age of around ~ 1.5 Gyr. This comparison with the results of the more traditional spectroscopic approach clearly supports the reliability of the optical/near-infrared photometric technique for analysing the stellar populations of early-type galaxies in distant clusters. Moreover, the photometric method requires

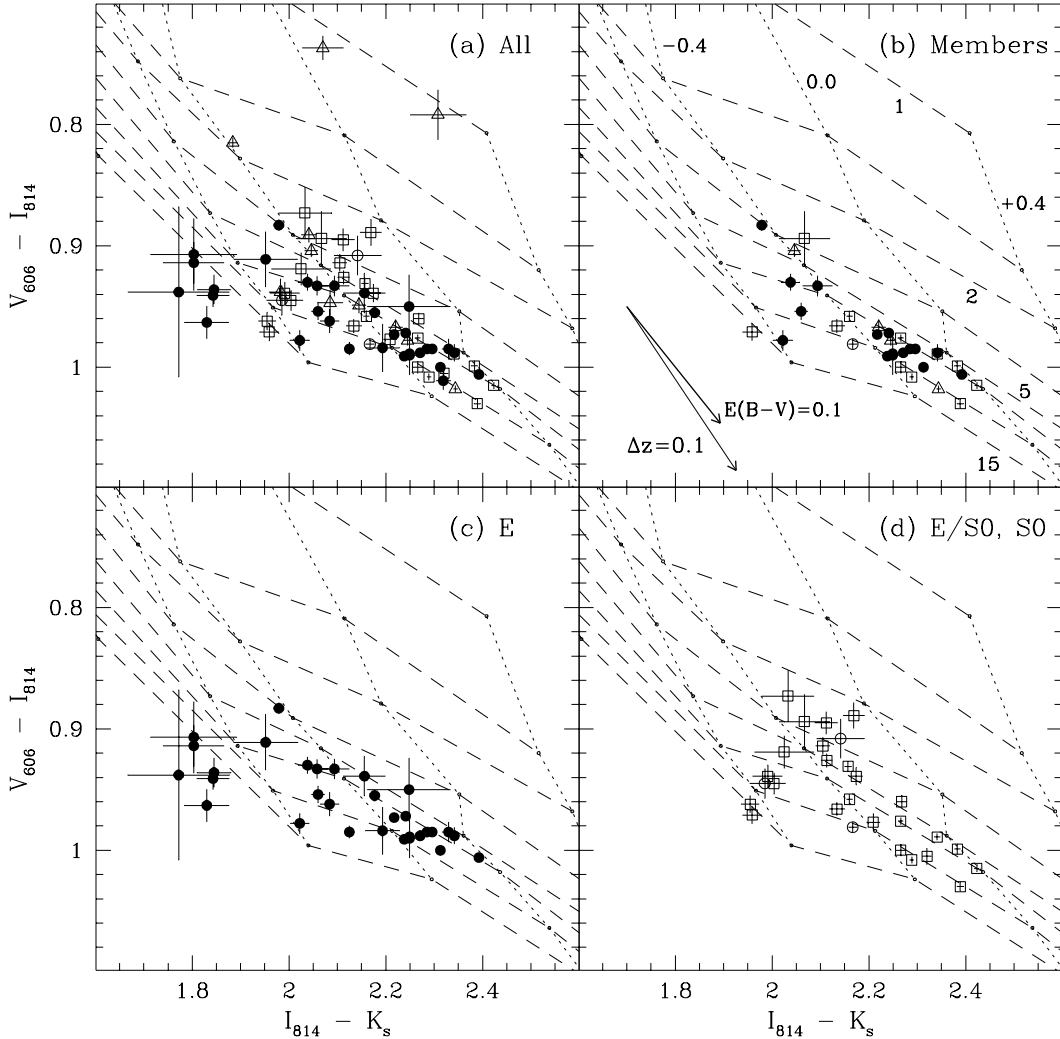


Figure 4. A mosaic of colour-colour plots illustrating their distribution in $(V_{606} - I_{814}) - (I_{814} - K_s)$ plane for the $K_s < 19$ sample. The points are coded on the basis of their optical morphology using the same symbols as Figure 3. The four panels show: a) the whole sample, b) just the spectroscopically-confirmed members; c) only the morphologically-typed ellipticals, d) only the morphologically classified S0s and E/S0. The relatively luminosities of the various galaxies can be gauged from the size of the errorbars on the data points.

only a fraction of the time needed for spectroscopic surveys and can probe to fainter luminosities.

Turning back to Figure 4 we now compare the colours of the different morphological subsamples. The sequence defined by the redder and more luminous galaxies appears in both the E and E/S0+S0 subsamples, as well as in the spectroscopically-confirmed members. There maybe a slight tendency for the bright E/S0+S0 sample to show a wider age spread than the E's ($\sigma_T(S0) = 2.2$ Gyrs versus $\sigma_T(E) = 0.8$ Gyrs at $K_s < 16.0$). The likelihood of this difference in dispersions arising by chance from the joint sample is only slight, $\log_{10}(P) = -3.1$. However, this comparison is very sensitive to the exact magnitude limit used.

Nevertheless, there is an even more striking difference between the two morphological subsamples at the lowest luminosities. To emphasise the variation in the properties

of the lowest luminosity galaxies we show in Figure 5 the colour-colour plot for the fainter ($K_s > 17$, $\lesssim 0.1L_K^*$) early-type galaxies. Here, while the faint ellipticals appear to extend the metallicity sequence defined by the brighter ellipticals (and S0's), the fainter S0 galaxies show an almost orthogonal colour-colour relationship to that exhibited by the faint ellipticals and all the more luminous galaxies (qualitatively similar behaviour is seen in the equivalent $(B_{450} - I_{814})$ plot). This reversal in the colour trends results from the appearance of a population of faint S0 with relatively blue ($V_{606} - I_{814}$) colours, indicating luminosity-weighted mean ages of only 2–5 Gyrs for the stellar populations in these galaxies and metallicities of $[M/H] \sim -0.2$. It is unlikely that all of the stars in these galaxies were formed in the most recent star formation event and hence the luminosity-

weighted ages are in fact upper limits on the epoch of the most recent star formation.

To quantify the prevalence of this population we arbitrarily define ‘young’ as a luminosity-weighted age of < 5 Gyrs and find that half of the $K_s > 17$ S0 galaxies are young (or 30% of the whole S0 population, Fig. 6), in contrast none of the faint E’s fall in this category. This is a high enough proportion of the S0 population (given the duration of the ‘young’ phase) to suggest that most of the faint lenticular galaxies in the cluster must have passed through this phase. To quantify the extent of any possible luminosity bias in our analysis we determine that the fading by the present-day of the stellar populations of the young S0 galaxies should not exceed 0.2 mags in K_s compared to the more luminous, evolved galaxies in the cluster (Smail et al. 1998; Kodama & Bower 2000). Taking this modest luminosity bias into account we find that it would reduce the proportion of ‘young’ S0s in an unbiased sample by only 5%.

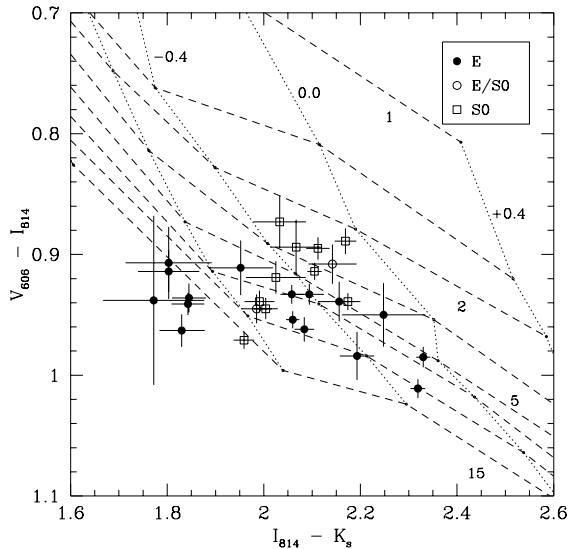


Figure 5. This plot compares the distribution of the faintest early-type galaxies ($K_s > 17$) in our sample to the predictions of the stellar population models. The striking difference in the distribution of faint E and S0 galaxies is obvious.

The behaviour exhibited by the faint lenticular population is very similar to that seen in the ‘UV+’ galaxies identified in a photometric survey of X-ray luminous clusters at $z \sim 0.2$ by Smail et al. (1998). Their relatively shallow ground-based imaging lacked the precision necessary for an analysis of the type undertaken here. Nevertheless, they used the increased sensitivity to differences in the stellar populations available from their ($U - B$) colours to identify a class of UV-bright galaxies which showed strong 4000Å breaks (‘UV+’) indicative of evolved stellar populations. They suggested that these UV+ galaxies represented the fading progenitors of the cluster S0 population. The UV+ class constitute around 50% of the faint cluster population ($< 0.1L_V^*$) which exhibit strong 4000Å breaks. Based on the *HST* imaging of a handful of the UV+ galaxies in the core of A 2390, Smail et al. (1998) suggest that the majority of these galaxies have S0 morphologies. The luminosities, colours and morphologies of the UV+ population are thus similar to the faint, blue S0 population identified here. Interestingly, Smail et al. (1998) found that the radial profile of the UV+ popu-

lation is indistinguishable from that of the luminous, evolved galaxies in these clusters suggesting that these galaxies are not recent additions to the cluster population.

We finally discuss the characteristics of the S0 population in the context of the morphological evolution discussed by Dressler et al. (1997) and Poggianti et al. (1999). The evolution in the number of S0 galaxies in clusters at $z > 0.3 - 0.6$ observed by Dressler et al. (1997) suggests that roughly two-thirds of the S0 population in a $z = 0.17$ cluster would have transformed their morphologies in the last 3 Gyrs (since $z \sim 0.5$), with half of these occurring in the last 1–2 Gyrs. Adopting a 1–2 Gyr delay between the termination of star formation and the morphological transformation occurring, as is needed to explain the lack of blue S0 galaxies in the distant clusters and the large number of passive galaxies with late-type morphologies (Poggianti et al. 1999; Kodama & Smail 2000), then we would expect that 60–70% of the S0 galaxies in A 2218 were forming stars 4–5 Gyrs prior to $z = 0.17$ and 30% of them within the last 2–3 Gyrs. To estimate the luminosity-weighted ages for the composite stellar populations in these galaxies at a later time we need to assume a model for their previous star formation. If we assume that these progenitors were forming stars at a constant rate (or slightly declining) since their formation at high redshift, as normal early and mid-type spiral galaxies are believed to do, then for the 30% of the S0 population which is predicted to have had terminated its star formation in the 2–3 Gyrs before $z = 0.17$ (equivalent to $z \sim 0.5$ in the cosmology we adopt) they would have luminosity-weighted ages of $\lesssim 5$ Gyrs when seen at $z = 0.17$. This model is thus consistent with the 30% fraction of the S0 population which we observe to have luminosity-weighted ages of $\lesssim 5$ Gyrs. Indeed, the smooth growth of the S0 fraction in the clusters reported by Dressler et al. (1997) is also mirrored by the nearly flat distribution of estimated ages for this population seen in Figure 6. Therefore, our observations support a scenario where the fraction of S0s in the clusters is smoothly increasing as a result of a slow morphological and spectroscopic transformation of star forming spiral galaxies into passive, S0 cluster members.

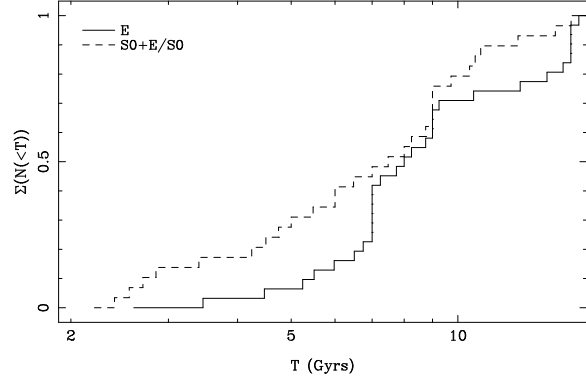


Figure 6. The cumulative distributions of the estimated luminosity-weighted relative ages of the full elliptical and lenticular samples. Note the relatively flat distribution of derived ages for the S0+E/S0 sample compared to the more uniform and older ages seen in the ellipticals, where the mean stellar populations in 80% of the galaxies are older than 7 Gyrs. We stress that these estimated ages should be viewed as relative rather than absolute values.

4 CONCLUSIONS

- We present precise optical and near-infrared photometry of a sample of 81 galaxies in the core regions of the rich cluster A 2218 at $z = 0.17$ (a lookback time of 3 Gyrs).
- We compare the optical and optical-infrared colours of the morphologically-classified early-type galaxies in our sample with the predictions of stellar population models spanning a range in metallicity and age. The models show good agreement in the regions of the colour-colour plane which are populated by the observational data.
- By comparing our results with those from a recent spectroscopic survey of the stellar populations in galaxies in A 2218, we confirm the reliability of the photometric analysis technique. We show that both techniques identify galaxies with relatively young stellar populations.
- The colours of the more luminous early-type galaxies ($\gtrsim 0.5L_K^*$) in the cluster are well described by a sequence of varying metallicity for the stellar population at a constant age. This is in agreement with the results of the analysis of the spectral line strengths in similar luminosity galaxies in A 2218 (Ziegler et al. 2000) and results from the spectroscopic and photometric analysis of galaxies in higher redshift clusters (Kodama & Arimoto 1997; Jones, Smail & Couch 2000).
- In contrast the faintest early-type galaxies ($\lesssim 0.1L_K^*$) show a large spread in their optical and optical-infrared colours. Around 30% of the S0 galaxies in A 2218 (and half of the fainter examples) exhibit mean luminosity-weighted ages for their stellar populations of $\lesssim 5$ Gyrs. This suggests that these galaxies were actively forming stars at $z \lesssim 0.5$. The proportion of these ‘young’ S0 galaxies is consistent with the rate of evolution of the S0 fraction in distant clusters reported by Dressler et al. (1997). Further support for the gradual growth of the S0 population comes from the relatively flat age distribution we derive for these galaxies. In contrast the vast majority of the morphologically-classified elliptical galaxies across all luminosities show evolved stellar populations.
- Most of the galaxies we see which show signs of recent activity lie below the magnitude limits reached by spectroscopic studies of galaxies in distant clusters. This highlights the urgent need to exploit the increased sensitivity available with 8-m telescopes to measure detailed line indices in low-luminosity members of intermediate and moderate redshift clusters.
- We have demonstrated the power of photometric analysis of the optical-infrared colours of early-type cluster galaxies to uncover information about their star formation histories. This type of precision photometric analysis should be extended to more distant clusters (in which it is predicted that a higher fraction of the S0 galaxies should show signs of past star formation activity) and to wider fields at intermediate redshifts to search for the signatures of the physical processes responsible for the spectroscopic and morphological transformations at the heart of the formation of S0 galaxies.

ACKNOWLEDGEMENTS

We thank Richard Bower, Warrick Couch, Roger Davies, Bianca Poggianti, Ray Sharples and Alex Vazdekis for useful conversations and help. IRS acknowledges support from

the Royal Society. HK and GPS acknowledge support from PPARC. TK acknowledges support through a Research Fellowship for Young Scientists from the Japan Society for the Promotion of Science.

REFERENCES

Aaronson, M., 1978, *ApJ*, 221, L103
 Aragon-Salamanca, A., Ellis, R.S., Couch, W.J., Carter, D., 1993, *MNRAS*, 262, 764
 Bertin, E., Arnouts, S., 1996, *A&AS*, 117, 393
 Bruzual, G., Charlot, S., 2000, in prep.
 Burstein, D., Heiles, C., 1982, *AJ*, 87, 1165
 Couch, W.J., Barger, A.J., Smail, I., Ellis, R.S., Sharples, R.M., 1998, *ApJ*, 497, 188
 van Dokkum, P.G., Franx, M., Kelson, D.D., Illingworth, G.D., Fisher, D., Fabricant, D., 1998, *ApJ*, 500, 714
 Dressler, A., Oemler, A., Couch, W.J., Smail, I., Ellis, R.S., Barger, A., Butcher, H., Poggianti, B.M., Sharples, R.M., 1997, *ApJ*, 490, 577
 Ellis, R.S., Smail, I., Dressler, A., Couch, W.J., Oemler, A., Butcher, H., Sharples, R.M., 1997, *ApJ*, 483, 582
 Fasano, G., Poggianti, B.M., Couch, W.J., Bettoni, D., Kjaergaard, P., Moles, M., 2000, *ApJ*, in press.
 Fruchter, A.S., Hook, R.N., 1997, in *Applications of Digital Image Processing*, ed A. Tescher, Proc. SPIE, 3164, 120
 Holtzman, J.A., Burrows, C.J., Casterno, S., Hester, J.J., Trauger, J.T., Watson, A.M., Worthey, G., 1995, *PASP*, 107, 1065.
 Jones, L.A., Smail, I., Couch, W.J., 2000, *ApJ*, 528, 118
 Jorgensen, I., Franx, M., Hjorth, J., van Dokkum, P.G., 1999, *MNRAS*, 308, 833
 Kelson, D.D., van Dokkum, P.G., Franx, M., Illingworth, G.D., Fabricant, D., 1997, *ApJ*, 478, 13
 Kelson, D.D., Illingworth, G.D., van Dokkum, P.G., Franx, M., 2000, *ApJ*, 531, 184
 Kneib, J.-P., Ellis, R.S., Smail, I., Couch, W.J., Sharples, R.M., 1996, *ApJ*, 471, 643
 Kodama, T., Arimoto, N., 1997, *A&A*, 320, 41
 Kodama, T., Arimoto, N., Barger, A., Aragon-Salamanca, A., 1998, *A&A*, 334, 99
 Kodama, T., Bower, R.G., 2000, *MNRAS*, submitted.
 Kodama, T., Smail, I., 2000, in prep.
 Kuntschner, H., 2000, *MNRAS*, 315, 184
 Le Borgne, F.J., Pello, R., Sanahuja, B., 1992, *A&AS*, 95, 87
 Moore, B., Lake, G., Katz, N., 1998, *ApJ*, 495, 139
 Packham, C., et al., 2000, in prep.
 Peletier, R., Balcells, M., 1996, *AJ*, 111, 2238
 Persson, S.E., Murphy, D.C., Kreminski, W., Roth, M., Rieke, M.J., 1998, *AJ*, 116, 2475
 Poggianti, B.M., Smail, I., Dressler, A., Couch, W.J., Barger, A.J., Butcher, H., Ellis, R.S., Oemler, A., 1999, *ApJ*, 518, 576
 Salpeter, E.E., 1955, *ApJ* 121, 161
 Schlegel, D., Finkbeiner, D.P., Davis, M., 1998, *ApJ*, 500, 525
 Smail, I., Dressler, A., Couch, W.J., Ellis, R.S., Oemler, A., Butcher, H., Sharples, R.M., 1997, *ApJS*, 110, 213
 Smail, I., Edge, A.C., Ellis, R.S., Blandford, R.D., 1998, *MNRAS*, 293, 124
 Smith, G.P., et al., 2000, in prep.
 Vazdekis, A., Arimoto, N., 1999, *ApJ*, 525, 144
 Vazdekis, A., Peletier, R.F., Beckman, J.E., Casuso, E., 1997, *ApJS*, 111, 203
 Worthey, G., 1994, *ApJS*, 95, 107
 Ziegler, B., Bower, R.G., Smail, I., Davies, R.L., Lee, D., 2000, *MNRAS*, submitted.

Table 1. Galaxy Catalogue

ID	ID ^a _{spec}	α, δ (J2000) 16 ^h , +66 ^o	K_s^{tot}	$(B_{450} - I_{814})$	$(V_{606} - I_{814})$	$(I_{814} - K_s)$	r_{hl} ($''$)	Morph	z	Note ^b
103	...	35 48.48, 12 1.7	17.72 ± 0.05	2.08 ± 0.03	0.79 ± 0.02	2.31 ± 0.06	1.05	Sdm	...	
129	...	35 46.60, 12 27.0	17.61 ± 0.03	2.33 ± 0.02	0.94 ± 0.01	1.98 ± 0.02	0.41	S0/a	...	
131	L404	35 48.80, 12 9.7	16.93 ± 0.02	2.31 ± 0.01	0.93 ± 0.01	2.04 ± 0.02	0.70	E	0.1708	
137	Z1516	35 46.84, 12 22.9	15.52 ± 0.01	2.44 ± 0.01	0.98 ± 0.00	2.24 ± 0.01	0.77	SB0/a	0.1638	
145	...	35 50.63, 12 1.9	16.82 ± 0.01	2.41 ± 0.01	0.95 ± 0.01	2.15 ± 0.01	0.53	Sab	...	
151	...	35 50.23, 12 5.6	18.24 ± 0.04	2.30 ± 0.02	0.94 ± 0.01	1.99 ± 0.03	0.37	E/S0	...	
153	...	35 52.49, 11 50.6	17.21 ± 0.02	2.55 ± 0.02	0.98 ± 0.01	2.33 ± 0.01	0.28	E	...	
154	B143	35 45.99, 12 32.9	16.54 ± 0.01	2.51 ± 0.01	0.99 ± 0.01	2.34 ± 0.01	0.43	E	0.1659	
159	...	35 45.02, 12 44.7	17.72 ± 0.03	1.95 ± 0.02	0.89 ± 0.01	2.17 ± 0.02	0.36	S0	...	
191	...	35 51.32, 12 7.6	17.30 ± 0.03	2.27 ± 0.02	0.90 ± 0.01	2.11 ± 0.02	0.62	S0	...	
195	...	35 44.97, 12 53.7	17.80 ± 0.05	2.27 ± 0.02	0.94 ± 0.01	1.84 ± 0.04	0.65	E	...	
205	B031	35 50.78, 12 20.5	15.21 ± 0.01	2.60 ± 0.01	1.03 ± 0.00	2.39 ± 0.01	0.75	S0	0.1835	
220	...	35 40.87, 12 36.7	17.08 ± 0.02	2.35 ± 0.01	0.94 ± 0.01	2.17 ± 0.01	0.52	S0	...	
230	...	35 47.60, 12 42.8	15.15 ± 0.01	2.54 ± 0.01	1.00 ± 0.01	2.32 ± 0.01	0.81	S0	...	
232	...	35 46.33, 12 52.0	15.39 ± 0.02	2.38 ± 0.01	0.96 ± 0.00	2.18 ± 0.01	0.80	E	...	
267	...	35 47.41, 13 5.3	17.96 ± 0.06	2.55 ± 0.03	0.98 ± 0.02	2.19 ± 0.03	0.23	E	...	
279	...	35 50.25, 12 19.6	16.47 ± 0.01	2.25 ± 0.01	0.93 ± 0.01	2.11 ± 0.01	0.69	S0	...	
280	B024	35 50.00, 12 23.8	14.37 ± 0.01	2.55 ± 0.01	1.02 ± 0.00	2.34 ± 0.00	1.03	SB0/a	0.1776	Z1552
285	L357	35 51.11, 12 34.1	16.77 ± 0.04	2.55 ± 0.02	0.99 ± 0.02	2.25 ± 0.02	0.32	E	0.1730	
292	L259	35 56.33, 11 51.1	15.11 ± 0.01	2.46 ± 0.01	0.98 ± 0.00	2.27 ± 0.01	0.91	S0	0.1646	
298	B020	35 49.47, 12 36.3	14.96 ± 0.01	2.42 ± 0.01	0.96 ± 0.00	2.16 ± 0.01	0.88	S0	0.1751	Z1580
301	K1	35 49.31, 12 44.7	13.19 ± 0.00	2.56 ± 0.00	0.97 ± 0.00	2.24 ± 0.00	3.50	E	0.1720	cD
303	B117	35 55.92, 12 3.4	16.98 ± 0.02	2.45 ± 0.02	0.98 ± 0.01	2.02 ± 0.02	0.69	E	0.1775	
307	B003	35 56.81, 11 55.5	13.77 ± 0.00	2.54 ± 0.00	0.99 ± 0.00	2.24 ± 0.00	2.84	E	0.1768	Z1437
315	B018	35 51.86, 12 34.3	14.55 ± 0.00	2.52 ± 0.01	1.01 ± 0.00	2.39 ± 0.00	0.71	E	0.1637	Z1662
323	...	35 59.05, 11 47.5	16.82 ± 0.01	2.28 ± 0.02	1.03 ± 0.01	2.64 ± 0.02	0.58	Sc	...	
324	...	35 54.90, 12 18.1	16.83 ± 0.02	2.23 ± 0.01	0.89 ± 0.01	2.04 ± 0.02	0.71	Sab	...	
326	B070	35 53.38, 12 38.6	16.03 ± 0.01	2.32 ± 0.01	0.90 ± 0.01	2.05 ± 0.01	1.16	Sab	0.1791	
333	B048	35 49.05, 13 0.8	15.64 ± 0.01	1.67 ± 0.01	0.82 ± 0.00	1.88 ± 0.01	0.92	Sc	0.1032	
337	B039	35 47.25, 13 16.1	15.20 ± 0.01	2.56 ± 0.01	0.99 ± 0.00	2.28 ± 0.01	0.78	E	0.1800	Z2604
350	...	35 43.50, 12 21.0	18.85 ± 0.08	2.28 ± 0.03	0.91 ± 0.02	2.14 ± 0.05	0.40	E/S0	...	
359	...	35 51.23, 12 55.0	17.23 ± 0.03	2.41 ± 0.02	0.96 ± 0.01	2.08 ± 0.02	0.53	E	...	
368	...	35 59.12, 12 1.3	16.86 ± 0.03	2.37 ± 0.02	1.21 ± 0.01	2.54 ± 0.02	0.70	Sc	...	
376	B064	35 57.43, 12 15.7	15.54 ± 0.01	2.55 ± 0.01	1.00 ± 0.00	2.38 ± 0.01	0.51	S0	0.1820	Z1454
380	...	35 51.06, 13 3.3	18.45 ± 0.10	2.47 ± 0.04	0.87 ± 0.02	2.03 ± 0.05	0.62	S0	...	
387	...	35 56.49, 12 27.1	18.79 ± 0.05	2.39 ± 0.03	0.96 ± 0.01	1.83 ± 0.05	0.27	E	...	
398	...	36 1.26, 11 55.8	17.93 ± 0.06	2.35 ± 0.03	0.94 ± 0.02	2.16 ± 0.04	0.56	E	...	
401	B030	35 59.42, 12 6.6	14.85 ± 0.01	2.51 ± 0.01	0.99 ± 0.00	2.27 ± 0.01	1.29	E	0.1798	Z1466
420	...	35 53.49, 12 57.2	16.52 ± 0.01	3.10 ± 0.03	1.21 ± 0.01	2.89 ± 0.01	0.82	Scd	...	
424	...	36 2.10, 11 58.4	18.93 ± 0.11	2.33 ± 0.03	0.91 ± 0.02	1.80 ± 0.06	0.33	E	...	
428	B028	36 2.33, 11 52.8	14.60 ± 0.00	2.60 ± 0.01	1.01 ± 0.00	2.42 ± 0.00	0.78	S0	0.1830	Z1343
439	...	36 0.57, 12 7.1	16.57 ± 0.02	2.48 ± 0.01	0.98 ± 0.01	2.21 ± 0.01	0.60	S0	...	
449	B087	35 56.72, 12 41.3	16.27 ± 0.01	2.17 ± 0.01	0.88 ± 0.00	1.98 ± 0.01	0.73	E	0.1717	Z1605
457	B121	35 54.67, 13 2.4	18.97 ± 0.10	2.42 ± 0.05	0.89 ± 0.02	2.07 ± 0.05	0.47	SB0/a	0.1717	
470	...	35 45.46, 12 8.5	17.16 ± 0.02	2.28 ± 0.01	0.91 ± 0.01	2.11 ± 0.01	0.43	S0	...	
503	B047	35 59.38, 12 53.6	15.38 ± 0.01	2.46 ± 0.01	0.97 ± 0.00	2.22 ± 0.01	0.79	E	0.1747	Z1711
537	Z2660	35 58.39, 13 21.5	16.05 ± 0.01	2.52 ± 0.01	0.98 ± 0.00	2.17 ± 0.01	0.73	E/S0	0.1773	
545	...	36 0.96, 13 10.2	18.76 ± 0.08	2.14 ± 0.03	0.92 ± 0.01	2.02 ± 0.06	0.83	S0	...	
563	B152	35 59.27, 13 33.8	17.16 ± 0.02	2.39 ± 0.01	0.95 ± 0.01	2.06 ± 0.01	0.40	E	0.1787	
571	...	36 0.00, 13 33.5	18.35 ± 0.06	3.12 ± 0.09	1.08 ± 0.03	2.96 ± 0.06	0.87	Scd	...	
599	B159	36 3.81, 13 14.3	17.32 ± 0.02	2.44 ± 0.01	0.97 ± 0.01	1.96 ± 0.02	0.53	S0	0.1731	
612	L143	36 2.64, 13 32.3	16.55 ± 0.02	2.44 ± 0.01	0.97 ± 0.01	2.13 ± 0.02	0.82	SB0/a	0.1811	
633	B017	36 4.25, 13 25.3	14.88 ± 0.00	2.57 ± 0.01	1.01 ± 0.00	2.29 ± 0.00	0.70	S0	0.1738	Z2702
634	...	36 4.40, 13 28.7	16.33 ± 0.01	2.48 ± 0.01	0.98 ± 0.01	2.13 ± 0.01	0.64	E	...	
638	...	36 3.81, 13 33.9	15.75 ± 0.01	2.31 ± 0.01	0.93 ± 0.00	2.16 ± 0.01	0.71	S0	...	
646	...	36 2.52, 13 50.8	18.32 ± 0.06	2.64 ± 0.05	1.28 ± 0.02	2.95 ± 0.05	0.56	Sdm	...	
647	...	36 4.75, 13 33.9	17.97 ± 0.03	2.36 ± 0.02	0.94 ± 0.01	1.84 ± 0.03	0.31	E	...	
660	...	35 43.40, 12 28.4	17.94 ± 0.04	2.36 ± 0.02	0.95 ± 0.01	2.09 ± 0.03	0.50	Sb	...	

a) Z: Ziegler et al. (2000), B: Butcher et al. (1983), L: Le Borgne et al. (1992), K: Kristian et al. (1978) – b) Ziegler et al. (2000).

Table 1. Galaxy Catalogue (cont)

ID	ID ^a _{spec}	α, δ (J2000) 16 ^h , +66°	K_s^{tot}	$(B_{450} - I_{814})$	$(V_{606} - I_{814})$	$(I_{814} - K_s)$	r_{hl} ($''$)	Morph	z	Note ^b
1018	...	36 0.43, 12 20.8	17.08 ± 0.03	2.34 ± 0.02	0.93 ± 0.01	2.06 ± 0.02	0.83	E	...	
1047	L187	36 0.34, 12 44.2	15.77 ± 0.01	2.51 ± 0.01	1.00 ± 0.00	2.31 ± 0.01	0.46	E	0.1750	
1057	B019	36 2.24, 12 34.5	14.57 ± 0.00	2.49 ± 0.01	0.99 ± 0.00	2.25 ± 0.00	1.27	E	0.1753	
1060	...	36 3.33, 12 32.6	17.36 ± 0.03	2.35 ± 0.02	0.94 ± 0.01	2.00 ± 0.02	0.41	S0	...	
1066	...	36 3.29, 12 36.7	17.51 ± 0.03	2.36 ± 0.02	0.94 ± 0.01	1.99 ± 0.03	0.71	S0	...	
2005	...	35 47.47, 12 24.2	18.53 ± 0.09	2.27 ± 0.04	0.91 ± 0.03	1.80 ± 0.09	0.44	E	...	
2010	...	35 49.18, 12 31.9	18.27 ± 0.13	2.28 ± 0.07	0.94 ± 0.07	1.77 ± 0.10	0.25	E	...	
2011	L389	35 49.32, 12 21.5	17.04 ± 0.04	2.26 ± 0.01	0.97 ± 0.01	2.22 ± 0.01	1.18	Sa	0.1800	
4001	...	36 3.40, 12 3.2	18.93 ± 0.08	1.20 ± 0.02	0.53 ± 0.01	1.42 ± 0.09	0.53	Sd	...	
4002	...	36 4.22, 12 12.0	15.99 ± 0.01	2.42 ± 0.01	0.96 ± 0.01	2.27 ± 0.01	0.92	S0	...	
4003	B185	36 3.54, 12 26.5	17.46 ± 0.03	2.32 ± 0.02	0.93 ± 0.01	2.09 ± 0.03	0.68	E	0.1821	
4004	...	36 6.45, 12 29.3	17.78 ± 0.03	> 5.0(2 σ)	3.00 ± 0.18	4.30 ± 0.04	0.29	?	...	
4005	...	36 6.56, 12 33.1	18.37 ± 0.04	> 4.1(2 σ)	1.97 ± 0.17	4.39 ± 0.08	0.36	Sc	...	
4006	...	36 5.97, 12 41.3	18.88 ± 0.08	2.40 ± 0.05	0.95 ± 0.03	2.25 ± 0.09	0.26	E	...	
4007	B036	36 6.41, 12 47.8	15.17 ± 0.01	2.52 ± 0.01	0.99 ± 0.00	2.34 ± 0.01	0.79	SB0	0.1681	
4008	...	36 5.64, 12 49.4	17.88 ± 0.04	1.54 ± 0.02	0.74 ± 0.01	2.07 ± 0.04	0.73	Sb	...	
4009	...	36 7.43, 13 0.3	16.36 ± 0.01	2.86 ± 0.02	1.12 ± 0.01	2.63 ± 0.01	0.73	Sa	...	
4010	B175	36 4.14, 13 2.2	17.07 ± 0.02	2.43 ± 0.02	1.01 ± 0.01	2.32 ± 0.02	0.43	E	0.2913	
4011	...	35 43.63, 13 9.6	18.79 ± 0.08	2.48 ± 0.04	0.91 ± 0.02	1.95 ± 0.07	0.50	E	...	
4012	...	36 6.71, 13 21.7	18.85 ± 0.06	3.73 ± 0.20	1.81 ± 0.05	3.69 ± 0.06	0.19	?	...	
4013	B015	35 44.12, 13 20.4	14.52 ± 0.00	2.57 ± 0.01	0.98 ± 0.00	2.30 ± 0.00	0.96	E	0.1778	
4014	Z2738	36 4.85, 13 42.5	16.22 ± 0.01	2.55 ± 0.01	1.00 ± 0.01	2.27 ± 0.01	0.46	S0	0.1742	
4015	...	36 9.28, 13 47.6	18.59 ± 0.04	2.57 ± 0.04	1.11 ± 0.02	2.58 ± 0.05	0.28	Sc	...	

a) Z: Ziegler et al. (2000), B: Butcher et al. (1983), L: Le Borgne et al. (1992), K: Kristian et al. (1978) – b) Ziegler et al. (2000).

This figure "fig1.jpg" is available in "jpg" format from:

<http://arxiv.org/ps/astro-ph/0008160v1>